

Radiative transfer in disc galaxies II – The influence of scattering and geometry on the attenuation curve

Maarten Baes^{*} and Herwig Dejonghe

Sterrenkundig Observatorium Universiteit Gent, Krijgslaan 281 S9, B-9000 Gent, Belgium, maarten.baes@rug.ac.be

8 April 2021

ABSTRACT

We investigate the influence of scattering and geometry on the attenuation curve in disc galaxies. We investigate both qualitatively and quantitatively which errors are made by either neglecting or approximating scattering, and which uncertainties are introduced due to a simplification of the star-dust geometry. We find that the magnitude of these errors depends on the inclination of the galaxy, and in particular that for face-on galaxies, the errors due to an improper treatment of scattering dominate those due to an imprecise star-dust geometry. Therefore we argue that in all methods which aim at determining the opacity of disc galaxies, scattering should be taken into account in a proper way.

Key words: radiative transfer – dust, extinction – galaxies: ISM

1 INTRODUCTION

During the last decade it has become clear that also in extragalactic astronomy, dust obscuration plays an important role, and that the construction of accurate galaxy models requires a proper radiative transfer modelling. However, it is often very time-consuming, and therefore practically unfeasible, to solve radiative transfer problems exactly. For example, assume we want to know the spatial distribution of stars and dust for a certain galaxy, where the only known data are observed surface brightnesses. The only means to solve this problem is to assume a certain parametrized model for the galaxy, containing a stellar and a dust component, and to solve the radiative transfer equation (RTE) for each set of parameters, and then select the model that fits the observations best. Such a modelling procedure demands an enormous number of RTE solutions, because the parameter space has to be sufficiently large in order to produce realistic models, in particular for disc galaxies (Misiriotis et al. 2000). Therefore it would be very useful if we could simplify the RTE in any way.

A first way to simplify the RTE is rather obvious: neglect the scattering term, which is responsible for the integro-differential character of the RTE (Christensen 1990, Jansen et al. 1994, Ohta & Kodaira 1995). However, already more than a decade ago, Bruzual et al. (1988) clearly demonstrate the importance of including scattering in radiative transfer calculations. Several other authors have since then confirmed these warnings, in particular Witt et

al. (1992). Another option to simplify the RTE is an approximation of the scattering term, by either forward or approximate isotropic scattering, or a combination of both (Natta & Panagia 1984, Guiderdoni & Rocca-Volmerange 1987, Calzetti et al. 1994). Di Bartolomeo et al. (1995) compare the attenuation curves calculated with these various approximate RTE solution methods, and find significant differences. Although these differences can partly be ascribed to different assumptions concerning the optical properties of the dust, it is very probable that also the approximate solution methods are responsible for a significant error.

It is obviously important to know the errors introduced on the attenuation curve by the various approximate solution techniques, but these have never been clearly determined. Either the approximate solutions are simply adopted without concern about the errors, or the errors are estimated for very simple galaxy models, such as homogeneous slabs or sandwich models (Bruzual et al. 1988, Di Bartolomeo et al. 1995). To make things worse, Disney et al. (1989) showed that the geometry of the stellar and dust distribution strongly determines the observed radiation field (without including the effects of scattering however). Lack of knowledge about the geometry can thus also introduce significant errors on the attenuation of galaxies.

In a previous paper (Baes & Dejonghe 2001, paper I) we described four different methods to solve the RTE in a plane-parallel geometry. These methods accommodate an arbitrary vertical distribution of stars and dust. We will now use these methods will allow us to address both issues of the RTE mentioned above. On the one hand, we can adopt them for a disc galaxy model with a realistic vertical structure, and compare the results with those obtained by us-

^{*} Research Assistant of the Fund of Scientific Research – Flanders (Belgium)

ing the various approximate solutions. This will allow us to quantify the errors introduced by the different approximations, and the importance of properly including scattering effects. On the other hand, we can apply these methods to a *family* of realistic galaxy models that can accommodate a wide range in distribution of stars and dust. This will allow us to investigate the influence of the geometry of the stellar and dust components on the attenuation curve, without any simplifying assumptions on the RTE such as the neglect of scattering. Last but not least, we can solve our RTE problems with four completely different methods: consistency is then a guarantee for accuracy.

In Section 2 we describe the radiative transfer mechanism and the ways to obtain the solution, and in Section 3, we present our set of disc galaxy models. In Section 4 and 5 we discuss respectively the influence of scattering and geometry on the attenuation curve as described above. In Section 6 we discuss the results.

2 RADIATIVE TRANSFER MODELS

2.1 The RTE in plane-parallel geometry

In plane-parallel geometry, the RTE can be written as

$$\mu \frac{\partial I}{\partial z}(z, \mu) = -\kappa(z)I(z, \mu) + \eta_*(z) + \frac{1}{2}\omega\kappa(z) \int_{-1}^1 I(z, \mu')\Psi(\mu, \mu')d\mu', \quad (1)$$

where $I(z, \mu)$ is the specific intensity of the radiation at a height z above the plane of the galaxy, and in a direction which makes an angle $\arccos \mu$ with the face-on direction $\mu = 1$. The known quantities in this equation are the dust opacity $\kappa(z)$, the stellar emissivity $\eta_*(z)$, the dust albedo ω and the angular redistribution function (hereafter ARF) $\Psi(\mu, \mu')$. The RTE can be brought in another form by introducing the optical depth τ instead of z ,

$$\tau(z) = \int_z^\infty \kappa(z')dz', \quad (2)$$

which yields

$$\mu \frac{\partial I}{\partial \tau}(\tau, \mu) = I(\tau, \mu) - S_*(\tau) - \frac{\omega}{2} \int_{-1}^1 I(\tau, \mu')\Psi(\mu, \mu')d\mu', \quad (3)$$

with $S_*(\tau) = \eta_*(\tau)/\kappa(\tau)$ is the stellar source function. This equation is to be solved for $0 \leq \tau \leq \tau_0$, the total optical (face-on) depth of the galaxy,

$$\tau_0 = \int_{-\infty}^\infty \kappa(z)dz. \quad (4)$$

Although the RTE can be solved for any point in the galaxy, we will focus on the attenuation $A(\mu)$, i.e. the fraction of the intensity that is attenuated by the dust detected by an observer at $\tau = 0$, into a certain direction μ . Because the RTE is a linear equation, this fraction will be independent of the total amount of stellar emission. We can thus choose the normalization of the stellar emissivity (or the source function). We take

$$\int_{-\infty}^\infty \eta_*(z)dz = \int_0^{\tau_0} S_*(\tau)d\tau = 1, \quad (5)$$

which means that the intensity that leaves the galaxy in the absence of dust in the face-on direction equals 1. In another direction μ , the dust-free intensity is then simply $1/\mu$ and the attenuation (in magnitudes) is

$$A(\mu) = -2.5 \log [\mu I(0, \mu)]. \quad (6)$$

2.2 Solution of the RTE

Because of the complexity of the RTE, a lot of authors have tried their ingenuity to find sophisticated methods to solve it. In paper I we presented four different methods to solve the RTE in plane-parallel geometry, which can handle absorption and multiple scattering, arbitrary vertical distributions of stars and dust and arbitrary phase functions.

(i) The spherical harmonics method consists of expanding all the angle-dependent terms in the RTE into a series of spherical harmonics, such that the RTE is replaced by a set of ordinary differential equations. The method turns out to be very efficient.

(ii) In the discretization method, originating from the theory of stellar atmospheres, integrals are replaced by sums and differentials by finite differences, resulting in a set of vector equations which can be solved iteratively.

(iii) In the iteration method, the intensity is expanded in a series of partial intensities. Each of the partial intensities obeys its own RTE, which can be solved iteratively. It can easily be extended to more complex geometries, but compared to the spherical harmonics method it is a very costly algorithm.

(iv) The Monte Carlo method is probably the most widely adopted method to solve radiative transfer problems, and the basic idea of the method consists of following the trajectory of a large amount of individual photons through the galaxy, whereby the fate of a photon on its path is determined by random events. For one-dimensional radiative transfer its efficiency is comparable to that of the iteration method.

For more details about these methods and references to the literature we refer to paper I. In this paper we will study the radiative transfer through a plane-parallel slab, as a function of the different physical and geometrical parameters. Having these four different methods to solve the RTE at our disposal proves to be very useful, not only to check the accuracy of the numerical results, as already mentioned, but also to understand the physical background of observed phenomena.

3 THE DISC GALAXY MODELS

In order to construct disc galaxy models we have to characterize the functions that appear in the RTE (1), i.e. specify the physical properties and spatial distribution of stars and dust. We will adopt a set of realistic galaxy models with a number of parameters. Varying these parameters will then enable us to investigate the influence of scattering and geometry on the attenuation curve. We will also adopt a template model to compare other models with.

Table 1. The adopted data sets for the optical properties of the dust grains. Tabulated are the optical depth τ relative to the V -band value, the scattering albedo ω and the asymmetry parameter g .

band	λ (μm)	τ	ω	g
UV1	125	3.44	0.42	0.60
UV2	150	2.75	0.42	0.59
UV3	175	2.44	0.48	0.58
UV4	200	2.87	0.48	0.54
UV5	225	3.01	0.51	0.46
UV6	250	2.38	0.57	0.46
UV7	300	1.92	0.57	0.47
U	360	1.60	0.57	0.49
B	440	1.32	0.57	0.48
V	550	1.00	0.57	0.44
R	700	0.73	0.54	0.37
I	850	0.47	0.51	0.31

3.1 The optical properties of the dust

Although it has been shown that the physical properties of dust in different environments can vary greatly (Witt et al. 1984, Mathis & Cardelli 1992), we will assume, for sake of simplicity, one single kind of dust grains. This means that the spatial and wavelength dependencies of all quantities appearing in (1) are separable. In particular, the dust albedo and the ARF are then independent of position.

To describe general anisotropic (conservative) scattering we adopt Henyey-Greenstein scattering (Henyey & Greenstein 1941). The ARF corresponding to this kind of scattering is a one-parameter function parametrized by the asymmetry parameter g , which is the average of the cosine of the scattering angle. A closed expression and a plot of the Henyey-Greenstein ARF can be found in Appendix A of Paper I. In Section 4 other kinds of scatterings such as forward and isotropic scattering, will be compared with Henyey-Greenstein scattering.

There are two ways to determine the wavelength dependence of the albedo ω , the asymmetry parameter g and the total optical depth τ_0 . On the one hand, values can be derived theoretically, by assuming a certain dust grain composition and calculating the optical properties of the dust (e.g. Draine & Lee 1984). On the other hand, optical properties can be derived empirically, usually based on a variety of observations of scattered light in the Galaxy (e.g. Bruzual et al. 1988). Our data set consists of the optical properties theoretically derived by Maccioni & Perinotto (1994), displayed in Di Bartolomeo et al. (1995). The adopted values are tabulated in table 1 for the central wavelengths of various bands.

3.2 The stellar distribution

The vertical distribution of stars in disc galaxies is still a matter of debate. The most straightforward way to derive such a vertical distribution is to study the surface brightness of edge-on galaxies at different heights above the plane. There is a general consensus that at great heights the light distribution decreases exponentially. Close to the plane of the galaxy however, dust attenuation makes the observation of the vertical distribution difficult. As a consequence, differ-

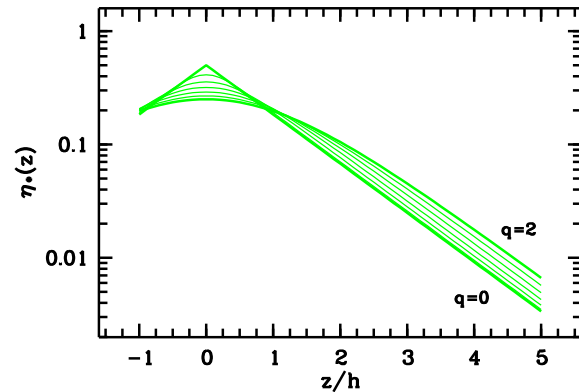


Figure 1. The stellar emissivity $\eta_*(z)$ of the family of sech^q models (7). It is shown for different values of the parameter q , ranging between the extreme values $q = 0$ and $q = 2$, which are indicated and plotted in bold. It is clear that they all have the same exponential asymptotic behaviour, whereas the sharpness of the peak at $z = 0$ is determined by q .

ent models have been proposed. The most popular models are an isothermal sheet distribution (van der Kruit & Searle 1981) and an exponential profile (Wainscoat et al. 1989). In order to allow a wide range in vertical density distributions, we adopt a two-parameter family of stellar emissivity profiles which were adapted from van der Kruit (1988),

$$\eta_*(z) = \frac{1}{q B\left(\frac{q}{2}, \frac{1}{2}\right) h} \text{sech}^q\left(\frac{z}{qh}\right), \quad (7)$$

where the function $B(x, y)$ in the represents the Beta function (Abramowitz & Stegun 1972). The first factor is determined such that the normalization condition (5) is satisfied. At great heights above the plane of the galaxy, the light distribution (7) indeed decreases exponentially,

$$\eta_*(z) \propto e^{-|z|/h} \quad \text{for } |z| \gg h. \quad (8)$$

The first parameter in (7) is the exponential scaleheight h . It is generally known that the velocity dispersion of different stellar types in the Galaxy is correlated with the age of the stars (e.g. Dehnen & Binney 1998). Due to this dynamical heating of the disc, the vertical scaleheight of the stars increases as a function of age (Wainscoat et al. 1992). Because the younger stellar populations are bluer than older ones, it can be expected that the scaleheight of stars increases with wavelength. Xilouris et al. (1999) accurately modelled several edge-on disc galaxies and found no significant trend of the stellar scaleheight with wavelength (from the blue to the near-infrared K band). Therefore we adopt a constant stellar scaleheight.

The second parameter in (7), q , corresponds to the $2/n$ used by van der Kruit (1988), and takes values between 0 and 2. It determines the shape of the stellar density near the plane of the galaxy, and hence is called the shape parameter. More precisely, the peak of the emissivity at $z = 0$ becomes sharper as q decreases. A number of emissivity profiles for various values of q is illustrated in Figure 1. For the special cases corresponding to the values $q = 0, 1$ and 2 , we find the

exponential, the sech- and the isothermal disc respectively,

$$q = 0 \quad \eta_*(z) = \frac{1}{2h} e^{-|z|/h} \quad (9)$$

$$q = 1 \quad \eta_*(z) = \frac{1}{\pi h} \operatorname{sech}\left(\frac{z}{h}\right) \quad (10)$$

$$q = 2 \quad \eta_*(z) = \frac{1}{4h} \operatorname{sech}^2\left(\frac{z}{2h}\right). \quad (11)$$

Although the sech^q profiles can be adopted for any value of q between 0 and 2 (e.g. de Grijs et al. 1997), it are these three models which are widely used in the literature to model the vertical structure in disc galaxies. For example, Schwarzkopf & Dettmar (2000) investigated the surface brightness of a set of 110 edge-on disc galaxies, and divided them into these three classes. They found that the intermediate sech-profile fitted the data (optical as well as near-infrared) best for 55% of the galaxies, whereas the exponential and isothermal profiles fitted 35% and 10% of the galaxies.

This would suggest to choose $q = 1$ as the typical value for our template model. However, in Section 5 we will demonstrate that the choice of q has only a minor effect on the attenuation curve, such that we are relatively free to choose q to our convenience. We choose an exponential profile $q = 0$ because it has some computational advantages (see Appendix A).

3.3 The dust distribution

Beside stars, we also need a dust component in the galaxy, which is determined by the opacity $\kappa(z)$. Again, the actual vertical distribution of dust in disc galaxies is difficult to investigate. Direct information about the distribution of dust can be obtained by spatially resolved far-infrared or submm observations, where the dust emission is directly observed. During the last years, several nearby spiral galaxies have been modelled at these wavelengths using ISO and SCUBA data (Haas et al. 1998, Alton et al. 1998a, 1998b, Davies et al. 1999, Domingue et al. 1999, Trewheella et al. 2000). For NGC 891, Alton et al. (2000) showed that the far-infrared emission in very good agreement with the dust distribution derived from radiative transfer calculations (Xilouris et al. 1998), where an exponential vertical dust profile was assumed.

It seems therefore obvious to assume that stars and dust have a similar distribution in the galaxy, but we allow the scaleheights to be different. We thus adopt a family of opacity functions

$$\kappa(z) = \frac{\tau_0}{q B\left(\frac{q}{2}, \frac{1}{2}\right) \zeta h} \operatorname{sech}^q\left(\frac{z}{q\zeta h}\right), \quad (12)$$

which satisfies the normalization condition (4). For our template model we will thus adopt an exponential model for both stars and dust. The quantity ζ represents the layering parameter, i.e. the ratio of the scaleheights of dust and stars (Disney et al. 1989).

Combining the emissivity (7) and the opacity (12) we can calculate the source function $S_*(\tau)$ for our galaxy mod-

els.* It is fairly straightforward to check that $S_*(\tau)$ will have the form

$$S_*(\tau) = \frac{1}{\tau_0} s_*\left(\frac{\tau}{\tau_0}, \zeta, q\right), \quad (13)$$

where $s_*(t, \zeta, q)$ is normalized as

$$\int_0^1 s_*(t, \zeta, q) dt = 1. \quad (14)$$

The source function hence does not depend on either of the scaleheights of the stellar or dust distribution, but only on their ratio ζ . Therefore the same is true for the attenuation $A(\mu)$, which will thus depend on two geometry parameters, the shape parameter q and the layering parameter ζ .

What is a representative value for the layering parameter? Normally, the interstellar matter sinks down to the central plane of a galaxy and forms an obscuring layer which is narrower than the stellar layer, such that $\zeta < 1$. This is observed in the Galaxy, where the scaleheights of the (thin) stellar disc and the dust disc are approximately 300 pc and 100 pc respectively. In edge-on galaxies dust lanes suggest that also there the dust distribution is narrower than the stellar one. Using detailed radiative transfer modelling for seven such galaxies, Xilouris et al. (1999) find that the dust scaleheight is about half that of the stars. For our template model we set $\zeta = 0.5$, but in Section 5 we will consider a wide range in ζ in order to investigate the dependence of the relative star-dust geometry on the attenuation.

The last parameter in our galaxy model is the total V band optical depth τ_V . Again, a realistic value for the optical depth in disc galaxies has been a subject of debate for a long time already. An extensive discussion can be found in e.g. Xilouris et al. (1997) and Kuchinski et al. (1998). The most widely supported idea is that spiral galaxies are transparent or moderately opaque if they are seen face-on, with a typical V band face-on optical depth of round unity. For our template model we adopt $\tau_V = 1$, which corresponds to an optical depth of 3 in the far UV and 0.5 in the I band (Table 1).

4 THE INFLUENCE OF SCATTERING

4.1 Approximations of the RTE

The RTE as written in (3) is a partial integro-differential equation, containing a differentiation along the path and an integration over the angle. The scattering term is the one that makes the RTE difficult, because this term is responsible for the coupling of the RTE along different paths: due to the integration over μ we cannot solve the RTE for different paths consecutively, but we have to solve it for all paths at the same time. Therefore it would be very practical if we could somehow get around the last term.

4.1.1 No scattering

One way is to neglect the scattered emission altogether, i.e. to take into account the photons that are removed from

* In Appendix A, we explicitly calculate the source function for the exponential model.

the beam, but neglect the photons that are added to the beam due to scattering. This is the same as assuming that all the interactions between dust grains and photons are absorption events, and hence that there are no scatterings. We will denote the resulting attenuation curve as the *ns* attenuation. Mathematically this translates into setting $\omega = 0$ (the albedo is the ratio of the scattering efficiency to the total extinction efficiency), such that the last term in (3) vanishes, which turns the RTE into an ordinary differential equation

$$\mu \frac{\partial I}{\partial \tau}(\tau, \mu) = I(\tau, \mu) - S_*(\tau). \quad (15)$$

With the appropriate boundary conditions it can directly be solved, and the *ns* attenuation becomes

$$A^{\text{ns}}(\mu) = -2.5 \log \int_0^{\tau_0} S_*(\tau) \exp\left(-\frac{\tau}{\mu}\right) d\tau. \quad (16)$$

A second way of getting around the scattering term is to neglect scattering completely, both the scattering absorption and the scattering emission. The photons that would normally be scattered out of the beam, are thus assumed to continue on their path. For the RTE this means that not only the last term vanishes (the photons added to the beam due to scattering), but also the fraction of the first term (the photons removed from the beam due to scattering). In this case the RTE becomes

$$\mu \frac{\partial I}{\partial \tau}(\tau, \mu) = (1 - \omega)I(\tau, \mu) - S_*(\tau). \quad (17)$$

This kind of interaction can also be described as completely *forward scattering*, because also then a scattering event has no net effect on a beam. The ARF for pure forward scattering is $\Psi(\mu, \mu') = 2\delta(\mu - \mu')$, and inserting this in (3) we find the same equation (17). This equation is readily solved, and the *fs* attenuation is

$$A^{\text{fs}}(\mu) = -2.5 \log \int_0^{\tau_0} S_*(\tau) \exp\left[-\frac{(1 - \omega)\tau}{\mu}\right] d\tau. \quad (18)$$

It is fairly straightforward to see that *fs* attenuation is in fact equivalent to *ns* scattering, but with the total optical depth replaced by an effective optical depth $\tau_{\text{eff}} = (1 - \omega)\tau_0$. If we thus obtain an expression for the *ns* attenuation, we immediately find the corresponding one for the *fs* attenuation.

4.1.2 (Approximate) isotropic scattering

In radiative transfer problems, much attention has always been paid to isotropic scattering. In some physical situations the assumption of isotropy can be correct. For example, according to Bruzual et al. (1988) and Corradi et al. (1996), the asymmetry parameter is close to zero in the near-infrared *K* band, such that scattering is virtually isotropic there.[†] Another useful situation where the assumption of isotropy can be applied is a medium where photons have a large probability to be scattered more than once, because multiple scattering tends to wash out the anisotropy effects. This principle has been applied by Vanevičius et al. (1997), who solve the

[†] Note however that this assumption is not always followed, e.g. Gordon et al. (1997) find $g_K = 0.43$.

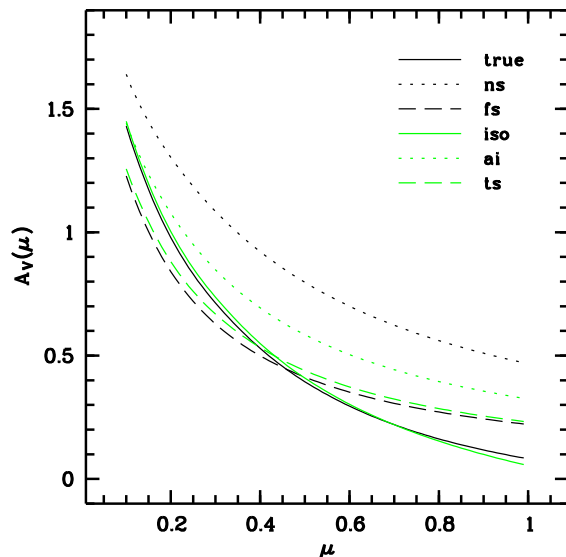


Figure 3. The V band attenuation curves $A(\mu)$ as a function of μ , corresponding to those in Figure 2.

RTE in a disc galaxy using the iteration method. For the first scattering they adopt the general anisotropic scattering, for the next scattering events isotropic scattering is assumed.

For isotropic scattering the distribution of the angles after a scattering event is uniform, such that the ARF is simply $\Psi(\mu, \mu') = 1$. A proper treatment of isotropic scattering hence does not change the integro-differential character of the RTE, and still requires the solution of the RTE for all path together. There are however two ways to approximate isotropic scattering such that the integration in the scattering term disappears.

The first possible approximation to isotropic scattering is the so-called isotropic two-stream approximation, introduced by Code (1973)[‡]. In the *ts* approximation a photon always remains on the same path, and after a scattering event it will either move in the same direction (i.e. forward scattering), or it moves in the opposite direction (i.e. reflection). The probability of forward scattering and reflection are equal. The ARF corresponding to this kind of scattering is thus infinitely peaked in two directions, and can be written as $\Psi(\mu, \mu') = \delta(\mu - \mu') + \delta(\mu + \mu')$. The intensity for a certain value of μ can then be found by solving the coupled set of RTEs

$$\begin{aligned} \mu \frac{\partial I}{\partial \tau}(\tau, \mu) &= \left(1 - \frac{\omega}{2}\right) I(\tau, \mu) - \frac{\omega}{2} I(\tau, -\mu) - S_*(\tau) \\ -\mu \frac{\partial I}{\partial \tau}(\tau, -\mu) &= \left(1 - \frac{\omega}{2}\right) I(\tau, -\mu) - \frac{\omega}{2} I(\tau, \mu) - S_*(\tau) \end{aligned} \quad (19)$$

For each inclination angle μ this set of ordinary differential

[‡] Code (1973) applied the two-stream approximation to calculate the flux escaping from a spherical dust envelope surrounding a star, and found a very good agreement with numerical results. He also proposes a second approximate solution, which works even better. However, this method cannot be applied to general plane-parallel (and other) geometries in a straightforward way, and is therefore not considered in this paper.

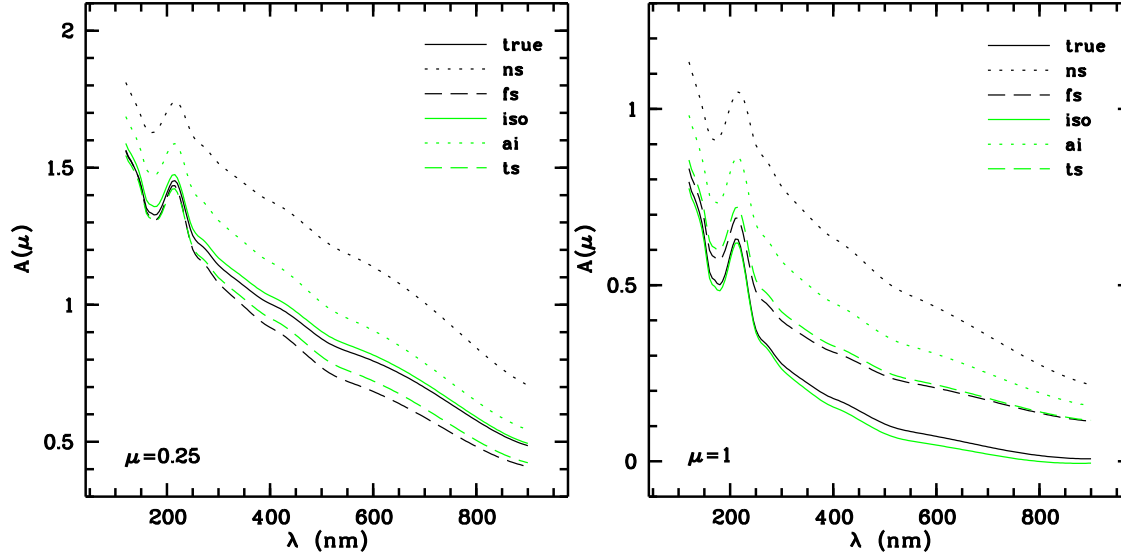


Figure 2. The various attenuation curves $A(\mu)$ as a function of wavelength. The left and right panel correspond to $\mu = 0.25$ and $\mu = 1$ respectively. The adopted model is the template model.

equations can be solved directly, such that we can calculate the two-stream attenuation curve $A^{\text{ts}}(\mu)$.

Another approximation for isotropic attenuation has been introduced by Natta & Panagia (1984), and afterwards adopted by various authors (e.g. Guiderdoni & Rocca-Volmerange 1987, Calzetti et al. 1994). Natta & Panagia (1984) suggest that a good approximation can be achieved by considering an attenuation equivalent to *ns* attenuation, but replacing the total optical depth by an effective optical depth $\tau_{\text{eff}} = \sqrt{1 - \omega} \tau_0$. The approximate isotropic attenuation or *ai* attenuation is thus

$$A^{\text{ai}}(\mu) = -2.5 \log \int_0^{\tau_0} S_*(\tau) \exp\left(-\frac{\sqrt{1 - \omega} \tau}{\mu}\right) d\tau. \quad (20)$$

Although there is no physical principle behind this approximation, it is attractive due to its simplicity.

4.2 Comparison of the attenuation curves

In the previous section we have described five approximations for the attenuation curve $A(\mu)$. These are compared in the Figures 2 and 3, where we plot them respectively as a function of wavelength for two different angles μ , and as a function of angle for the *V* band.

4.2.1 Scattering versus no scattering

We first compare the attenuation curve with the *ns* approximation, i.e. the situation where the scattering emission is neglected. Qualitatively, the difference between the *ns* and all other attenuation curves is obvious: by not taking into account the scattered emission, the attenuation is overestimated in all directions. Because the probability of scattering is slightly higher than the probability of absorption at optical wavelengths (see Table 1), it will be no surprise that this overestimation compared to the true attenuation can

be considerable. In particular for face-on directions, we obtain a difference of nearly half a magnitude for our template model. Only for high inclinations, the *ns* approximation is more or less satisfactory.

Another way to understand the effect of scattering is to compare the true attenuation curve with the *fs* attenuation curve, i.e. the situation where scattering is neglected completely. Particularly in Figure 3 the effect of including scattering on the attenuation curve is clearly observable: the attenuation becomes larger for small μ and smaller for large μ . The overall effect of scattering is thus apparently that photons are removed from lines of sight with a high inclination and sent into face-on directions, where they leave the galaxy. This is due to the fact that the optical depth along a path with inclination μ is proportional to $1/\mu$. Photons that initially (or after a scattering event) move on a path with large inclination have a large possibility to interact with a dust grain. If they are scattered into a direction which is nearly face-on, the probability to interact with another dust grain is much smaller, such that they can easily leave the galaxy.

This overall effect of scattering is responsible for a rather strange behaviour for face-on galaxies. If we look carefully at the right panel in Figure 2, we see that the true face-on attenuation becomes zero at the *I* band. The loss of radiation due to absorption (0.2 mag \approx 20 per cent) is thus completely balanced by the gain due to scattering. This is not due to some particular properties of the dust at the *I* band, but only to the smaller optical depth. When we consider a smaller total optical depth, the extinction can even be negative, i.e. a face-on galaxy can be brighter than it would be without dust. This is illustrated in Figure 4, where we plot the face-on attenuation in the *V*-band as a function of the total optical depth. Using the iteration method such that the contribution of each partial intensity can be considered separately. The attenuation corresponding to the photons that leave the galaxy directly, i.e. the *ns* attenuation, is of

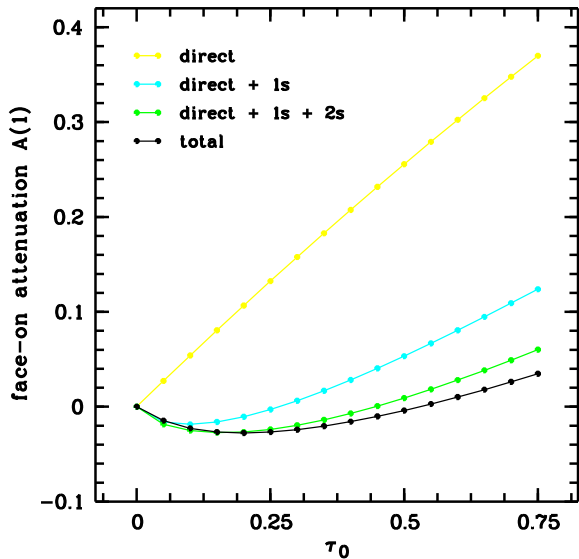


Figure 4. The V band face-on attenuation $A(1)$ as a function of the total optical depth τ_0 . Shown are the attenuation corresponding to photons that leave the galaxy directly, directly or after one scattering (direct + 1s), directly or after one or two scatterings (direct + 1s + 2s), and the total attenuation. Except for the varying total optical depth, the galaxy models have the same parameters as our template model ($q = 0$ and $\zeta = 0.5$.)

course positive everywhere. But adding the photons which leave the galaxy after one scattering event, the attenuation already is negative for $\tau_0 < 0.25$. The total attenuation remains negative for $\tau_0 < 0.5$, a result in correspondence with Bruzual et al. (1988) and Di Bartolomeo et al. (1995).

4.2.2 Anisotropic versus isotropic scattering

At first sight one would expect a significant difference between the isotropic and the anisotropic attenuation curves. First, at optical and UV wavelengths the anisotropy parameter is fairly large ($g \sim 0.5$), and for these wavelengths the Henyey-Greenstein phase function is far from isotropic (e.g. Bianchi et al. 1996, Figure 2). Second, the total optical depth in our galaxy model is only moderate, such that the anisotropy effects should not be washed out by multiple scattering. However, Figure 2 and 3 show that the isotropic attenuation approximates the anisotropic attenuation very well, with differences between both attenuation curves only a few hundredths of a magnitude.

In Figure A1 of Paper I we plotted the Henyey-Greenstein ARF for various values of μ' . For nearly face-on lines-of-sight μ' , the distribution of the new angles μ is far from uniform. For very inclined lines-of-sight however, the ARF is fairly uniform, due to the averaging out over all azimuths. For photons which are scattered from such lines-of-sight, the scattering seems thus approximately isotropic. In our galaxy model, the majority of the scattering events occurs on paths which are nearly edge-on, because along such paths the optical depth is much larger than on paths which are nearly face-on. This explains why even for the moderate optical depth of our galaxy, the differences between the isotropic and anisotropic attenuation are fairly small.

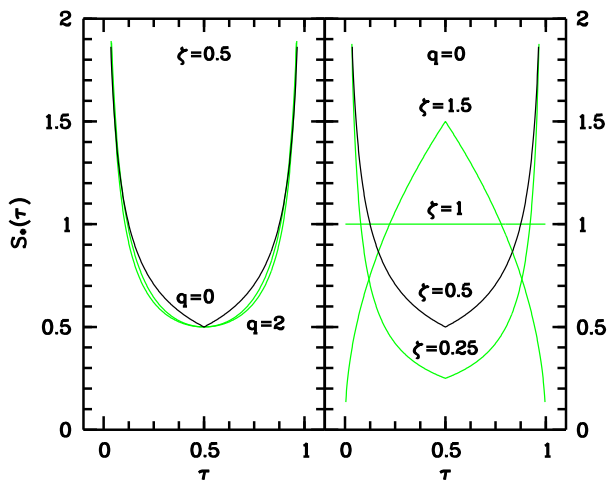


Figure 5. The source function $S_*(\tau)$ of the family of sech^q models as a function of the parameters q and ζ . In each of the panels the template model is the black curves, and we vary one of the geometry parameters. *Left:* variation of the shape parameter q , taking the values 0, 1 and 2. *Right:* variation of the layering parameter ζ , taking the values 0.25, 0.5, 1 and 1.5.

As mentioned, there is little gain in the observation that the isotropic attenuation curve approximates the true anisotropic one so well, because the approximation does not simplify the RTE. However, if the ts or ai attenuation curves were to be satisfying approximations for the isotropic attenuation curve, the operational gain would be significant. Unfortunately, the Figures 2 and 3 show that the approximations are not satisfying. The two-stream approximation is both qualitatively and quantitatively comparable to the fs approximation, i.e. an overestimation of the attenuation in face-on directions of more than 0.1 mag, and an underestimation of the same order for highly inclined directions. The ai attenuation curve lies between the ns and fs attenuation curve, which is logical if we compare the expressions (16), (18) and (20). This means that the approximation is satisfying for highly inclined directions, but the attenuation is severely overestimated in the face-on direction ($\Delta A \approx 0.25$ mag).

5 THE INFLUENCE OF GEOMETRY

Our models contain two parameters which specifically determine the geometry of the galaxy model: the shape parameter q determines the *actual distribution* of stars and dust near the galaxy plane, whereas the layering parameter determines the *relative distribution* of stars and dust. In this section we investigate to which degree these geometry parameters determine the attenuation curve of the galaxy.

5.1 The shape parameter q

The RTE (3) shows that the source function completely determines the attenuation curve, i.e. once $S_*(\tau)$ is known, we can calculate $A(\mu)$. Therefore, if we want to know the influence of q on the attenuation curve it is interesting to firstly study its influence on the source function. In Figure 5

we plot $S_*(\tau)$ for various models with different shape parameters. The source function depends only weakly on the parameter q , more precisely the shape of S_* becomes slightly rounder at the centre of the galaxy as q increases. It seems logical to predict a similar insensitivity on q for the attenuation curves. This is confirmed by our calculations. Even the differences between the attenuation curves of the two extreme cases, the exponential disc and the isothermal sheet, are almost negligibly small.

5.2 The layering parameter ζ

The layering parameter is the ratio of the scaleheights of dust and stars and hence determines the relative distribution of the two components. Variation of this parameter yields a wide range of dust-stars geometries. This can be seen in Figure 5, where the source function is plotted for various models with different layering parameter ζ . According to the shape of the source function for a particular value of ζ , we can classify the different geometries into three classes.

For $\zeta = 1$, the stars and dust have the same scaleheight and thus the same spatial distribution. The source function is then independent of the depth in the galaxy, and due to the normalization (5) we find $S(\tau) = 1/\tau_0$. In general, each galaxy model with a similar distribution of stars and dust will have such a constant source function. Because the attenuation curve is completely determined by the source function only, all galaxy models with a similar distribution of stars and dust will be equivalent. In particular, our model will be equivalent to the *homogeneous slab*, i.e. a finite galaxy model with stars and dust homogeneously mixed. Such a model has been considered by many authors (e.g. Bruzual et al. 1988, Calzetti et al. 1994, Di Bartolomeo et al. 1995) as an approximation of a disc galaxy.

For $\zeta < 1$ the dust has a smaller scaleheight than the stars, such that the attenuation will predominantly occur in the central regions. As mentioned in Section 3.3, this is the most realistic range for the layering parameter. If $\zeta < 1$, the source function has its minimal value in the centre of the galaxy, and diverges at the edges. If ζ tends to zero, the dust will form an infinitely thin obscuring layer in the central plane of the galaxy. We will refer to this model as the *thin dust disc* model.

For $\zeta > 1$ the dust has a larger scaleheight than the stars, and the attenuation will thus occur relatively more in the outer regions of the galaxy. The source function is then maximal in the centre of the galaxy, and vanishes at the edges of the galaxy. If ζ grows larger, the bulk of the dust attenuation will occur further away from the central plane of the galaxy. In the limit $\zeta \rightarrow \infty$ the dust is infinitely thinly distributed over all space, and will effectively behave as a set of two obscuring layers on both sides of the galaxy. This geometry, where the obscuring material is located only between the observer and the source, is known as the *overlying screen* model. It is the analogue of attenuation of stars in the Galaxy. Various authors advise against the use of this model (Disney et al. 1989, Witt et al. 1992).

The source function is thus strongly dependent on the relative distribution of stars and dust, whereas the actual shape of the distribution is only of minor importance. We will now investigate in detail whether this also means that

the influence of the layering parameter on the attenuation curve is significant.

5.2.1 Effects on the *fs* attenuation curve

First we will only consider true absorption and neglect scattering, and we will hence investigate the influence of ζ on the *fs* attenuation curve. For the exponential model $q = 0$, the source function is fairly simple, and the integration (18) can be performed analytically. One finds

$$A^{\text{fs}}(\mu) = 0.543 \frac{(1-\omega)\tau_0}{\mu} - 2.5 \log \mathcal{W}_\zeta \left[\frac{(1-\omega)\tau_0}{2\mu} \right]. \quad (21)$$

This expression is derived in Appendix A, and the definition and some properties of the function $\mathcal{W}_\zeta(x)$ are described in Appendix B. The advantage of the expression (21) is that it easily allows us to study the attenuation curve as a function of ζ . For every value of x , $\mathcal{W}_\zeta(x)$ is a decreasing function of ζ , moderately decreasing for small x and strongly decreasing for large x . This implies that $A^{\text{fs}}(\mu)$ will be an increasing function of ζ . The more extended the dust distribution, relative to the stellar one, the larger the attenuation and thus the fainter the galaxy appears. In particular, the overlying screen model is the most efficient and the thin dust disc the least efficient absorbing geometries. This behaviour is illustrated in Figure 6a, where we plot the *fs* attenuation curve $A^{\text{fs}}(\mu)$ as a function of μ for a set of layering parameters ζ . For highly-inclined directions (small values of μ) the *fs* attenuation changes considerably as a function of the layering parameter.

5.2.2 Effects on the true attenuation curve

Let us now investigate the influence of ζ on the true attenuation curve, which has to be calculated numerically. In Figure 6b the results are shown: we see a different behaviour between the *fs* and the true attenuation curves. Whereas the *fs* attenuation is an increasing function of ζ in all directions, the true attenuation is not: for small inclination angles, the true attenuation decreases as a function of ζ . This difference is also illustrated in Figure 6c, where we plot the *fs* and true attenuation explicitly as a function of the layering parameter for different inclination angles. The *fs* curves all rise, whereas the true attenuation curve rises for small values of μ , but decreases in the face-on direction $\mu = 1$.

If scattering is not taken into account, galaxies with an extended dust distribution are more efficiently obscured than galaxies with their dust concentrated in the central region. However, if scattering is taken into account, the efficiency turns around for face-on directions. *In face-on directions, galaxies with their dust concentrated in the central region are more efficiently obscured than galaxies with an extended dust distribution.* How can this be understood physically? In Section 4 we showed that scattering biased the preferential direction for photons to leave the galaxy: it is easier to leave it face-on than for highly-inclined directions. In particular photons which are scattered near the edge of the galaxy are responsible for this: if a photon is scattered there into a face-on direction, its probability to leave the galaxy without another interaction is high. Now, the more extended the dust distribution in the galaxy, the more dust is in the outer regions, and the more photons which

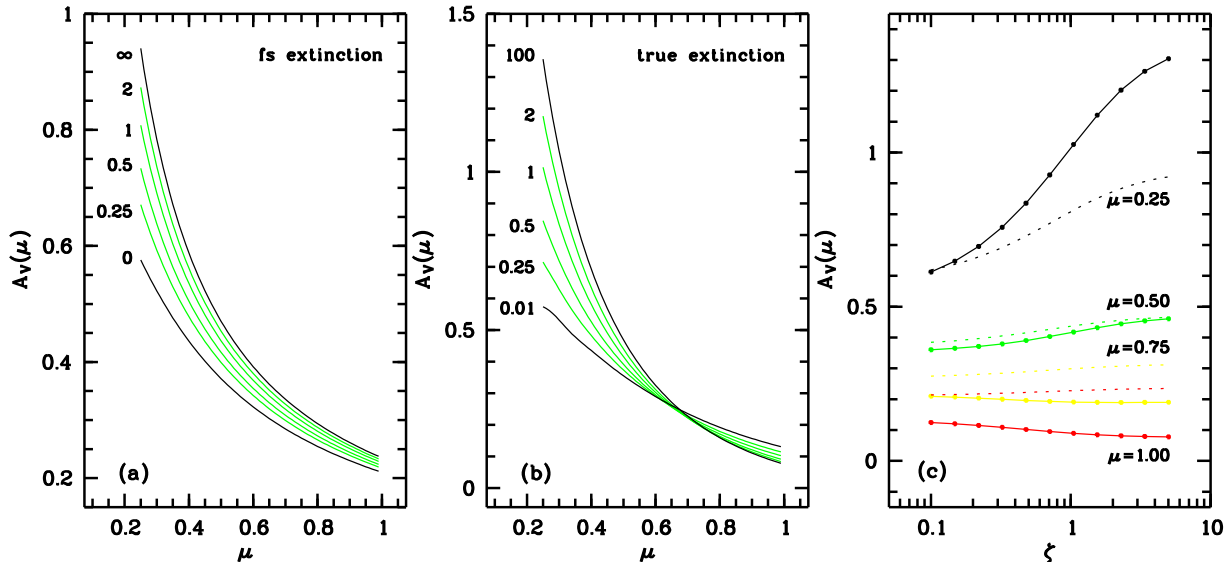


Figure 6. (a.) The *fs* attenuation $A_V(\mu)$ curve as a function of μ for some different values of the layering parameter ζ , which are indicated. The black curves denoted by $\zeta = 0$ and $\zeta = \infty$ correspond to the thin dust disc and overlying sheet models respectively. (b.) Same as a., but now the true attenuation curve. (c.) The true and *fs* attenuation curves $A_V(\mu)$ as a function of the layering parameter ζ . The solid lines represent the true attenuation curve, the dotted lines are the *fs* attenuation curves. The results are shown for four angles, which are indicated.

are scattered out of the galaxy in nearly face-on directions. Relative to galaxies with concentrated dust, galaxies with an extended dust distribution on the one hand efficiently absorb photons and on the other hand they scatter a considerable amount of photons in the face-on direction.

Which of these two effect dominates is determined by the total optical depth. For small optical depths the scattering effect will be more important, and $A(\mu)$ will decrease with increasing ζ for nearly-face-on directions. In contrary, for large optical depths, the absorption will dominate and $A(\mu)$ will be an increasing function of ζ . We can thus conclude that

- inclined galaxies with a moderate optical depth are most efficiently obscured if the dust is more extended than the stars.
- nearly face-on galaxies with a moderate optical depth are most efficiently obscured if the dust is concentrated in the central regions.
- optically thick galaxies are most efficiently obscured if the dust is more extended than the stars.

Notice that the difference between small and large optical depth can also be considered for one single galaxy, when we study the attenuation as a function of wavelength. This is shown in Figure 7, where we plot the attenuation curve as a function of wavelength for two angles μ and for three models with a different layering parameter. For a total *V* band optical depth $\tau_V = 1$, the attenuation behaves as an optically thick galaxy at the blue side of the spectrum, and as an optically thin galaxy in the red wavelength range, with the crossover between the two regimes occurs around 300 nm ($\tau_0 \approx 2$).

These results can be compared with those found by Bruzual et al. (1988), who adopted a sandwich model (i.e. a

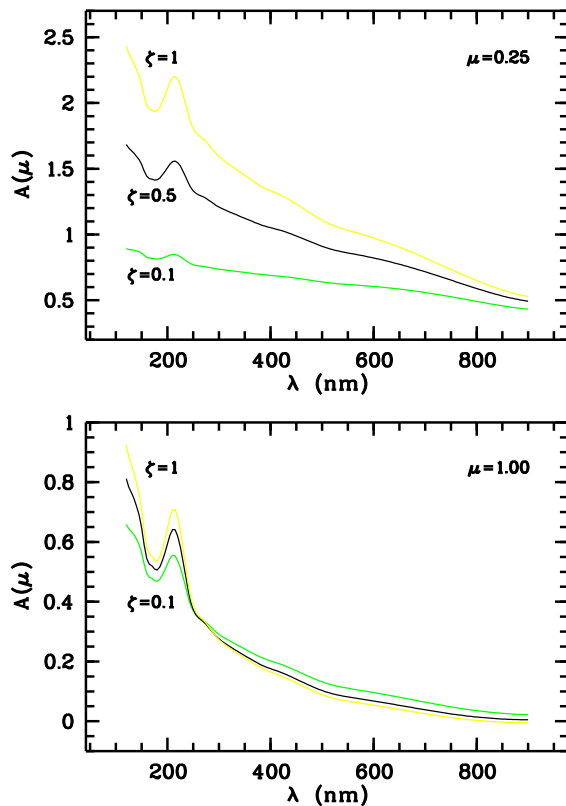


Figure 7. Three attenuation curves $A(\mu)$ as a function of wavelength for three models with a different layering parameter. The values for ζ are 0.1, 0.5 and 1, the other parameters are those of the template model ($\tau_V = 1$ and $q = 0$). The upper panel and the lower panel correspond to $\mu = 0.25$ and $\mu = 1$ respectively.

slab where stars and dust are homogeneously mixed, surrounded on both sides by a slab containing stars only). They varied the relative thicknesses of the slabs, and found a similar result of the dependence of the attenuation curve on the layering parameter (only shown for the face-on direction $\mu = 1$). Bruzual et al. (1988) concluded that the differences in the attenuation curve between the various models have the same order of magnitude than the uncertainties due to an imprecise knowledge of the optical parameters of the dust, and hence that a homogeneous slab is a satisfying model for disc galaxies. We agree that in the face-on direction, quantitatively the difference in attenuation between centrally concentrated and extended distributions is of the order $\Delta A \approx 0.1$ mag for optical wavelengths. These differences become even smaller if we constrain the range of ζ to realistic values. The layering parameters obtained by Xilouris et al. (1999) all lie between 0.30 and 0.75 at optical wavelengths, and for these values $\Delta A(\mu)$ is only of the order of a few hundredths mag. Also for moderately inclined galaxies, the attenuation curve will not seriously depend on ζ if it this parameter is constrained to a realistic range. Only if the optical depth is considerably higher, due to (a combination of) a larger amount of dust, a more opaque wavelength region or a large inclination, the uncertainty of the relative geometry of dust and stars causes a considerable uncertainty on the attenuation.

6 DISCUSSION AND CONCLUSION

The aim of this paper was to investigate how the RTE can be simplified and what errors are introduced by doing so. More than a decade ago already, Bruzual et al. (1988) investigated to the effects of scattering on the attenuation in disc galaxies (albeit for a simple plane-parallel model), and Disney et al. (1989) showed that the adopted geometry of the galaxy model strongly influences the attenuation (without taking scattering into account however). We wanted to reexamine these effects in detail and in the same manner, i.e. within a realistic set of disc galaxy models and properly taking multiple scattering into account.

In Section 4 we showed that the nature of the physical process of scattering is such that it connects different lines of sight with each other. The overall effect of scattering is that many photons which originally move on a inclined line-of-sight, leave the galaxy in the face-on direction. Any approximate method to simplify the RTE where photons cannot leave their initial path (such as the *ns*, *fs*, *ts* and *ai* approximations described in Section 4), will not be able to reproduce this behaviour. In particular for face-on galaxies, the optical depth will always be underestimated by such approximations, as illustrated in Figure 2. If we compare the attenuation curves corresponding to isotropic and anisotropic scattering however, we see that the difference between them are only of the order of a hundredth of a magnitude. Anisotropy effects are essentially washed out. Inversely it will be impossible to determine an ARF from photometry.

The effects of scattering are also important if we investigate the influence of the star-dust geometry on the attenuation in disc galaxies. If scattering is not taken into account, as in Disney et al. (1989), we find that the atten-

uation is more effective if the dust distribution is extended. For a same amount of dust, the larger the layering parameter, the larger the attenuation. In particular this means that the overlying screen geometry is the most efficient obscuring geometry, whereas galaxies with a dust scaleheight smaller than the stellar scaleheight, are less efficiently obscured. However, when scattering is taken into account, this picture does not hold anymore. We find the remarkable effect of scattering that in the face-on direction, galaxies with a moderate optical depth ($\tau_0 < 2$) are most efficiently obscured by a centrally concentrated dust distribution. This is very interesting because the optical depth of spiral galaxies is thought to be of the order unity in optical bands.

The effects of scattering and geometry not only need to be investigated in a qualitative way, it is important to know them quantitatively. This allows us to answer questions as how large our error is when we approximate anisotropic scattering by assuming it is forward, or when we assume a dust scaleheight equal to that of the stars, where in reality it is only half of it.

The magnitude of these errors depends on the inclination. In the face-on direction, the errors induced by not properly taking scattering into account are largest. In the *ns* approximation, the induced errors rise up to nearly half a magnitude, for forward scattering they are of the order of 0.15 mag at optical wavelengths (Figure 2b). The errors introduced by uncertainty about the star-dust geometry are only of the order of a few hundredths of a magnitude (Figure 7b), and thus significantly smaller. For inclined directions, the optical depth along lines-of-sight towards the observer is much larger. The attenuation curve then becomes less dependent on the angular redistribution function, in agreement with Di Bartolomeo et al. (1995). The differences between the attenuation curves corresponding to different star-dust geometries grows significantly. For example, for a galaxy with an inclination of 75° ($\mu = 0.25$), the differences between the true, isotropic, forward and two-stream attenuation curves become about 0.1 mag at optical wavelengths, and only a few hundredth of a magnitude in the UV (Figure 2a). However, assuming a homogeneous slab model instead of our template model, the induced error on the attenuation curve is about 0.3 magnitudes at optical and more than half a magnitude at UV wavelengths. For face-on galaxies it is thus important to include scattering in a proper way in the modelling, for inclined galaxies it is important to have a fairly good idea of the star-dust geometry of the galaxy.

In the light of the adopted models, two remarks are appropriate. (1) By working in plane-parallel geometry we have the advantage that we could use four independent methods to solve the RTE, such that the accuracy of the obtained results can be checked carefully. We are well aware of the fact that plane-parallel galaxy models do not represent very realistic galactic discs. More detailed modelling requires an exponential fall-off in the radial direction (Freeman 1970), a distinction in attenuation between arm and interarm regions (e.g. White et al. 2000), and an inclusion of the effects of clumping of both stars and dust (Witt & Gordon 1996, 2000; Bianchi et al. 2000). Nevertheless we are convinced that our modelling can contribute to the understanding of the mechanism of radiative transfer, and we have all reasons to believe that our results would hold qualitatively in more complex models. (2) We know that scattering and geometry

are not the only two elements that introduce uncertainties to the attenuation of disc galaxies. In Article I we solved the RTE for identical galaxy models, but with two different sets of optical dust parameters found in the literature. We obtained differences between the attenuation curves of the order of a few tenths of a magnitude. Uncertainty about the optical properties of the dust hence also introduces errors to the attenuation curve. However, these errors are independent of those introduced by an inaccurate treatment of scattering or geometry, and they hence do not affect the conclusion of this work.

As a final remark, we re-iterate a warning that has also been issued by others: do not use too simplistic models to determine the opacity in disc galaxies. There are many ways to investigate the amount of attenuation or the optical thickness of disc galaxies. Following Xilouris et al. (1997), we can divide them into two categories, the small N approach and the large N approach. The small N approach tries to determine the opacity of individual nearby disc galaxies by constructing detailed radiative transfer models. Obviously, these methods would reveal wrong results if scattering is neglected. The large N approach aims at determining a mean value for the optical depth in disc galaxies, by statistically studying a large sample of galaxies. Of such a sample of galaxies a certain observable is then compared to a galaxy model, in order to derive the optical depth. However, these methods are difficult to interpret because of selection effects (Davies et al. 1993), and there are often model-dependent. For example, Saunders et al. (1990) estimate an average effective optical depth of disc galaxies by fitting a screen model to the optical and far-infrared luminosity functions. Trewhella et al. (1997) redid these calculations with a sandwich model, and found a very different conclusion. We want to stress that also in such studies the effects of scattering need to be taken into account, because they are, except for very inclined galaxies, at least as important as the effects of geometry. An often used prescript to take scattering into account, is to determine an effective optical depth τ_{eff} for a galaxy model without scattering and compensate the obtained value for scattering. These compensations are simply multiplications, such as $\tau_0 = \tau_{\text{eff}}/(1-\omega)$ or $\tau_0 = \tau_{\text{eff}}/\sqrt{1-\omega}$, which can but not necessarily need to have a physical justification. With our paper we hope to have clearly showed that such approximations are not able to accurately reproduce the effects of scattering. We therefore argue that scattering needs to be accounted for properly in statistical studies concerning the opacity of disc galaxies.

REFERENCES

Abramowitz M., Stegun I. A., 1972, Handbook of Mathematical Functions, Dover Publication Inc., New York
 Alton P. B., Trewhella M., Davies J. I., Evans R., Bianchi S., Gear W., Thronson H., Valentijn E., Witt A., 1998a, A&A, 335, 807
 Alton P. B., Bianchi, S., Rand R. J., Xilouris E. M., Davies J. I., Trewhella M., 1998b, ApJ, 507, L125
 Alton P. B., Xilouris E. M., Bianchi S., Davies J., Kylafis N., 2000, A&A, 356, 795
 Baes M., Dejonghe H., 2001, submitted to MNRAS [paper I]
 Bianchi S., Ferrara A., Giovanardi C., 1996, ApJ, 465, 127

Bianchi S., Ferrara A., Davies J. I., Alton P. B., 2000, MNRAS, 311, 601
 Bruzual A. G., Magris C. G., Calvet N., 1988, ApJ, 333, 673
 Calzetti D., Kinney A. L., Storchi-Bergmann T., 1994, ApJ, 429, 582
 Christensen J. H., 1990, MNRAS, 246, 535
 Code A. D., 1973, in *Interstellar Dust and Related Topics*, Greenberg J. M. and van de Hulst H. C. eds., Reidel, Dordrecht, p. 505
 Corradi R. L. M., Beckman J. E., Simonneau E., 1996, MNRAS, 282, 1005
 Davies J. I., Phillips S., Boyce P. J., Disney M. J., 1993, MNRAS, 260, 491
 Davies J. I., Alton P., Trewhella M., Evans R., Bianchi S., 1999, MNRAS, 304, 495
 Dehnen W., Binney J. J., MNRAS, 298, 387
 de Grijs R., Peletier R. F., van der Kruit P. C., 1997, A&A, 327, 966
 Di Bartolomeo A., Barbaro G., Perinotto M., 1995, MNRAS, 277, 1279
 Disney M., Davies J., Phillipps S., 1989, MNRAS, 239, 939
 Domingue D. L., Keel W. C., Ryder S. D., White R. E. III, 1999, AJ, 118, 1542
 Draine B. T., Lee H. M., 1984, ApJ, 285, 89
 Freeman K. C., 1970, ApJ, 160, 811
 Gordon K. D., Calzetti D., Witt A. N., 1997, ApJ, 487, 625
 Guiderdoni B., Rocca-Volmerange B., 1987, A&A, 186, 1
 Jansen R. A., Knapen J. H., Beckman J. E., Peletier R. F., Hes R., 1994, MNRAS, 270, 373
 Haas M., Lemke D., Stickel M., Hippelein H., Kunkel M., Herbstmeier U., Mattila K., 1998, A&A, 338, L33
 Henyey L. G., Greenstein J. L., 1941, ApJ, 93, 70
 Kuchinski L. E., Terndrup D. M., Gordon K. D., Witt A. N., 1998, AJ, 115, 1438
 Maccioni A., Perinotto M., 1994, A&A, 284, 241
 Mathis J. S., Cardelli J. A., 1992, ApJ, 398, 610
 Misiriotis A., Kylafis N. D., Papamastorakis J., Xilouris E. M., 2000, A&A, 353, 117
 Natta A., Panagia N., 1984, ApJ, 287, 228
 Ohta K., Kodaira K., 1995, PASJ, 47, 17
 Saunders W., Rowan-Robinson M., Lawrence A., Efstathiou G., Kaiser N., Ellis R. S., Frenk, C. S., 1990, MNRAS, 242, 318
 Schwarzkopf U., Dettmar R.-J., 2000, A&A, 361, 451
 Trewhella M., Davies J. I., Disney M. J., Jones H. G. W., 1997, MNRAS, 288, 397
 Trewhella M., Davies J. I., Alton P. B., Bianchi S., Madore B. F., 2000, ApJ, 543, 153
 Vasevičius V., Arimoto N., Kodaira K., 1997, ApJ, 474, 623
 van der Kruit P. C., 1988, A&A, 192, 117
 van der Kruit P. C., Searle L., 1981, A&A, 95, 105
 Wainscoat R. J., Freeman K. C., Hyland A. R., 1989, ApJ, 337, 163
 Wainscoat R. J., Cohen M., Volk K., Walker H. J., Schwartz D. E., 1992, ApJS, 83, 111
 White R. E. III, Keel W. C., Conselice C. J., 2000, ApJ, 542, 761
 Witt A. N., Bohlin R. C., Stecher T. P., 1984, ApJ, 279, 698
 Witt A. N., Gordon K. D., 1996, ApJ, 463, 681
 Witt A. N., Gordon K. D., 2000, ApJ, 528, 799
 Witt A. N., Thronson H. A. Jr., Capuano J. M. Jr., 1992, ApJ, 393, 611
 Xilouris E. M., Kylafis N. D., Papamastorakis J., Paleologou E. V., Haerendel G., 1997, A&A, 325, 135
 Xilouris E. M., Alton P., Davies J., Kylafis N. D., Papamastorakis J., Trewhella M., 1998, A&A, 331, 894
 Xilouris E. M., Byun Y., Kylafis N. D., Paleologou E. V., Papamastorakis J., 1999, A&A, 344, 868

APPENDIX A: THE EXPONENTIAL MODEL

In this appendix we take a closer look at the exponential model $q = 0$, characterized by

$$\eta_*(z) = \frac{1}{2h} e^{-|z|/h} \quad (\text{A1})$$

$$\kappa(z) = \frac{\tau_0}{2\zeta h} e^{-|z|/\zeta h}. \quad (\text{A2})$$

Disney et al. (1989) already considered a similar galaxy model (their Triplex model). They managed to calculate an expression for the observed intensity if scattering is not taken into account. We will derive the solution of the RTE by direct integration of the formal solution (16). Therefore we first need an explicit expression for the source function $S_*(\tau)$. The optical depth is obtained by combining (A2) with (2),

$$\tau(z) = \begin{cases} \frac{\tau_0}{2} \left[2 - \exp\left(\frac{z}{\zeta h}\right) \right] & \text{for } z \leq 0 \\ \frac{\tau_0}{2} \exp\left(-\frac{z}{\zeta h}\right) & \text{for } z \geq 0, \end{cases} \quad (\text{A3})$$

and inverting this relation we obtain

$$z(\tau) = \begin{cases} -\zeta h \ln(2t) & \text{for } 0 \leq t \leq \frac{1}{2} \\ -\zeta h \ln[2(1-t)] & \text{for } \frac{1}{2} \leq t \leq 1, \end{cases} \quad (\text{A4})$$

where $t = \tau/\tau_0$ is the relative optical depth. Introducing this expression in (A1) and (A2) we find an expression for the stellar source function $S_*(\tau)$,

$$S_*(\tau) = \begin{cases} \frac{\zeta}{\tau_0} (2t)^{\zeta-1} & \text{for } 0 \leq t \leq \frac{1}{2} \\ \frac{\zeta}{\tau_0} [2(1-t)]^{\zeta-1} & \text{for } \frac{1}{2} \leq t \leq 1. \end{cases} \quad (\text{A5})$$

The source function is of the form (13), and the normalization condition (14) is satisfied. The fact that $S_*(\tau)$ has a fairly simple power law form, will allow us to calculate an expression for the ns attenuation, by direct integration of the formal solution (16). Inserting $S_*(\tau)$ in (16) we obtain

$$A^{\text{ns}}(\mu) = 0.543 \frac{\tau_0}{\mu} - 2.5 \log \zeta \int_0^1 x^{\zeta-1} \cosh\left[\frac{\tau_0}{2\mu}(x-1)\right] dx, \quad (\text{A6})$$

which becomes, using the function $\mathcal{W}_\zeta(x)$ defined as in Appendix B,

$$A^{\text{ns}}(\mu) = 0.543 \frac{\tau_0}{\mu} - 2.5 \log \mathcal{W}_\zeta\left(\frac{\tau_0}{2\mu}\right), \quad (\text{A7})$$

This result is in agreement with the solution obtained by Disney et al. (1989). Knowing this expression, we immediately also have an expression for the fs and ai attenuation curves

$$A^{\text{fs}}(\mu) = 0.543 \frac{(1-\omega)\tau_0}{\mu} - 2.5 \log \mathcal{W}_\zeta\left[\frac{(1-\omega)\tau_0}{2\mu}\right] \quad (\text{A8})$$

$$A^{\text{ai}}(\mu) = 0.543 \frac{\sqrt{1-\omega}\tau_0}{\mu} - 2.5 \log \mathcal{W}_\zeta\left(\frac{\sqrt{1-\omega}\tau_0}{2\mu}\right). \quad (\text{A9})$$

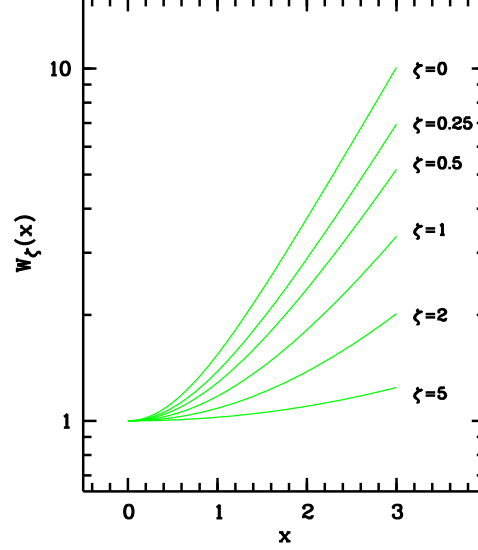


Figure B1. The function $\mathcal{W}_\zeta(x)$ as a function of x for different values of ζ .

APPENDIX B: THE FUNCTION $\mathcal{W}_\zeta(x)$

For $\zeta > 0$ and for all values of x , we define the function $\mathcal{W}_\zeta(x)$ by the integral

$$\mathcal{W}_\zeta(x) = \zeta \int_0^1 (1-t)^{\zeta-1} \cosh(xt) dt. \quad (\text{B1})$$

For natural values of ζ , the integral can immediately be solved in terms of elementary functions, for example

$$\mathcal{W}_1(x) = \frac{\sinh x}{x} \quad (\text{B2})$$

$$\mathcal{W}_2(x) = 2 \frac{\cosh x - 1}{x^2} \quad (\text{B3})$$

$$\mathcal{W}_3(x) = 6 \frac{\sinh x + x}{x^3}. \quad (\text{B4})$$

For non-integer values of ζ the integral can be calculated by expanding the cosh function,

$$\begin{aligned} \mathcal{W}_\zeta(x) &= \zeta \sum_{k=0}^{\infty} \frac{1}{(2k)!} x^{2k} \int_0^1 (1-t)^{\zeta-1} t^{2k} dt \\ &= \sum_{k=0}^{\infty} \frac{\Gamma(\zeta+1)}{\Gamma(\zeta+2k+1)} x^{2k} \end{aligned} \quad (\text{B5})$$

$$= 1 + \frac{x^2}{(\zeta+1)(\zeta+2)} + \frac{x^4}{(\zeta+1)(\zeta+2)(\zeta+3)(\zeta+4)} + \dots \quad (\text{B6})$$

Using d'Alembert's convergence theorem one can easily show that this power series converges absolutely. It can be written as a hypergeometric function,

$$\mathcal{W}_\zeta(x) = {}_1F_2\left(1; \frac{\zeta+1}{2}, \frac{\zeta+2}{2}; \frac{x^2}{4}\right). \quad (\text{B7})$$

Considering the expansion (B5) we can also consider the special cases $\zeta = 0$ and $\zeta = \infty$,

$$\mathcal{W}_0(x) = \cosh x \quad (\text{B8})$$

$$\mathcal{W}_\infty(x) = 1. \quad (\text{B9})$$

In Figure B1 we plot $\mathcal{W}_\zeta(x)$ as a function of x for a few values of ζ . It is an even function of x , increasing for positive x , the minimal value being $\mathcal{W}_\zeta(0) = 1$ for all ζ . Regarded as a function of ζ for fixed values of x , $\mathcal{W}_\zeta(x)$ it is a decreasing function, depending weakly on ζ for small x and strongly for large x .

This paper has been produced using the Royal Astronomical Society/Blackwell Science L^AT_EX style file.